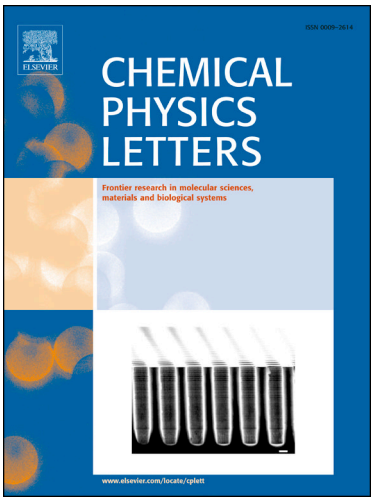

Research paper

Time Resolved Study of Hydroxyl Radical Oxidation of Oleic Acid at the Air-Water Interface

Xinxing Zhang, Kevin M. Barraza, Kathleen T. Upton, J.L. Beauchamp

PII: S0009-2614(17)30499-2
DOI: http://dx.doi.org/10.1016/j.cplett.2017.05.051
Reference: CPLETT 34840

To appear in: *Chemical Physics Letters*

Received Date: 24 March 2017
Revised Date: 18 May 2017
Accepted Date: 19 May 2017

Please cite this article as: X. Zhang, K.M. Barraza, K.T. Upton, J.L. Beauchamp, Time Resolved Study of Hydroxyl Radical Oxidation of Oleic Acid at the Air-Water Interface, *Chemical Physics Letters* (2017), doi: http://dx.doi.org/10.1016/j.cplett.2017.05.051

Time Resolved Study of Hydroxyl Radical Oxidation of Oleic Acid at the Air-Water Interface

Xinxing Zhang, Kevin M. Barraza, Kathleen T. Upton, and J. L. Beauchamp*

Noyes Laboratory of Chemical Physics and the Beckman Institute, California Institute of Technology, Pasadena, California, 91125

*Electronic Mail: jlbchamp@caltech.edu

Telephone: +001-6263956525

Abstract

The ubiquity of oleic acid (OA) renders it a poster child for laboratory investigations of environmental oxidation chemistry. In the current study, mechanistic details of the oxidation of OA by hydroxyl radicals at the air-water interface are investigated using field-induced droplet ionization mass spectrometry (FIDI-MS). Products from OH oxidation of both unsaturated and saturated carbon atoms are identified, and mechanisms for both types of oxidation processes are proposed. Uptake of oxygen in the interfacial layer increases linearly with time, consistent with Langmuir-Hinshelwood reaction kinetics. These results provide fundamental knowledge relating to OH initiated degradation of fatty acids in atmospheric aerosols.

Introduction

Fatty acids are pervasive in nature. Being surfactants, they tend to exist at oil-water or air-water interfaces. They widely occur in many kinds of oils[1,2] and living organisms.[3,4] Due to this ubiquity, fatty acids such as oleic acid (OA) are found on the surfaces of atmospheric aerosols formed by sea spray[5-8] and result from anthropogenic activities like cooking.[9,10] In the atmosphere, interfacial reactions associated with the oxidation of organics are of major interest because resultant secondary organic aerosols (SOA) are known to have adverse impacts on climate, human health, atmospheric chemistry in general and organic aerosols in particular. Hence, the degradations of fatty acids due to interfacial chemistry, especially interfacial oxidation reactions, are very important environmental processes.

Differences in the oxidative behaviors between saturated and unsaturated fatty acids center around the C=C double bond. Oxidation of airborne organics are mainly initiated by reaction with ozone (O_3), nitrate radical (NO_3), and hydroxyl radical (OH).[11] Ozone selectively reacts with unsaturated C=C bonds, but behaves inert towards saturated hydrocarbons. In contrast, NO_3 and OH react with both saturated and unsaturated hydrocarbons, with the rate coefficients for oxidation of unsaturated hydrocarbons being significantly larger than for oxidation of corresponding saturated molecules.[11] This is reasonable in the sense that the C=C double bond is considered to be electron-rich while oxidation is essentially an electron flow to the oxidizers. Among these three oxidizers, the OH radical is especially interesting because it is responsible for initiating oxidative degradation of most trace species in the lower atmosphere,[12] with the deserved reputation of being the "atmosphere's detergent". The OH oxidation of saturated hydrocarbons is initiated by abstraction of an H atom, resulting in an alkyl radical and a

water molecule. Unsaturated hydrocarbons, on the other hand, can undergo addition of OH to the C=C bond, yielding a nascent β-hydroxylalkyl radical.[11]

OA has become a model system used to study the atmospheric oxidation of fatty acids not only because it contains both saturated and unsaturated carbon atoms, but also because field studies have demonstrated that OA is the most prevalent unsaturated fatty acid observed in the amphiphilic coats of marine aerosols, and it is also highly abundant in tropospheric particulate matter.[8,9] Further, the oleoyl group of OA is one of the most prevalent unsaturated hydrophobic chains found in phospholipids. To date, the oxidation of OA by ozone at the air-water interface has been studied by field-induced droplet ionization mass spectrometry (FIDI-MS),[13] sum frequency generation vibrational spectroscopy,[14] and by monitoring other surface properties such as surface tension and surface pressure.[15,16] The NO_3, OH and ozone oxidation studies of oleic acid particles were also performed using flow tube reactors,[17-20] chamber studies,[21] attenuated total reflectance infrared spectroscopy,[22] as well as aerosol mass spectrometry.[23] In these studies, the products, mechanism, and kinetics of oleic acid oxidation by various oxidizers have been examined. However, to the best of our knowledge, no detailed studies of OH mediated oxidation of oleic acid at the air-water interface has been reported.

Recently, our group pioneered the technique field-induced droplet ionization mass spectrometry (FIDI-MS).[24-27] This interface-sensitive technique employs a soft ionization method to sample ions from the surface of microliter liquid droplets using a pulsed critical electric field, for analysis by mass spectrometry. In the current study, we couple the FIDI-MS technique with a steady flow of OH radicals generated from a dielectric barrier discharge source (DBDS). By varying the exposure time of the hanging droplet to the DBDS, we obtain the time-dependence of product yield at the droplet surface. We observe that the C=C double bond of OA is always

oxidized first, with further oxidation products of both the saturated and unsaturated carbon atoms containing five or more oxygen being identified by mass spectrometry. To clarify the mechanism of saturated hydrocarbon oxidation, similar experiments are performed with the saturated analog stearic acid to compare with the results for OA. By postulating the oxidation mechanisms, we aim to provide a model system to understand the OH oxidation of amphiphiles at the air-liquid interface.

1. Methods

1.1 Chemicals and reagents

Oleic acid (≥ 99%) and stearic acid (≥ 98.5%) were purchased from Sigma Aldrich (St. Louis, MO, USA) and used without further purification. All solvents (water and methanol) are HPLC grade and purchased from EMD Chemicals Inc. (Gibbstown, NJ, USA). A 2 mM solution is firstly obtained by dissolving oleic acid and stearic acid in methanol as the stock solution, and then diluted to 100 μM by water for experimental use.

1.2 Air-water interfacial oxidation by OH

The FIDI-MS instrument has been described in detail elsewhere.[24] Briefly, a hanging droplet of ~2 mm o.d. (~4 μL in volume) is suspended on the end of a stainless steel capillary between two parallel plate electrodes separated by 6.3 mm. Droplets are formed from liquid fed through the capillary using a motorized syringe pump. The parallel plates are mounted on a translation stage to allow alignment of an aperture in the electrically grounded plate with the atmospheric pressure inlet of an LTQ-XL mass spectrometer (Thermo-Fisher, Waltham, MA). The capillary is mounted on a separate translation stage to place the droplet exactly midway between the two plates and to align with the inlet of the LTQ-XL. Mass spectrometric sampling of the hanging

droplet is accomplished by applying a pulsed high voltage (typically -3 to -5 kV, 100 ms duration) to the back parallel plate and to the capillary at half the magnitude applied to the back plate to maintain field homogeneity between the front and back plate. When a sufficiently high voltage is applied, the electrical forces overcome the surface tension of the droplet, resulting in the bipolar ejection of highly-charged progeny droplets less than 1 μm in diameter from the opposite ends of the suspended droplet.[24,28] Charged droplets of a specific polarity enter the transfer capillary of the mass spectrometer, resulting in the detection of gas-phase ions. In this case, we apply negative voltage on the back plate in order to detect the deprotonated oleic acid and stearic acid anions and their oxidation products. After each droplet is formed, we allow 60 seconds for the molecules to diffuse to the air-water interface before exposing the droplet to hydroxyl radicals for a variable reaction time typically up to 60 s. Amphiphile concentrations, kept below the critical micelle concentration (CMC) limit, are sufficient to insure formation of a monolayer with a subsurface excess. After the OH oxidation, we trigger the high voltage to sample both reactants and products. Sampling occurs on a millisecond time scale.

2.3 Dielectric Barrier Discharge Source (DBDS)

Hydroxyl radicals are generated using a dielectric barrier discharge source (DBDS) composed of a borosilicate tube (1/4" OD, 3/16" ID) which acts as the dielectric material. A tungsten filament inner electrode is sealed within the tube, and a conductive silver epoxy coating (McMaster-Carr, Santa Fe Springs, CA, USA) acts as an outer electrode. A glass bubbler provides water saturated helium through the DBDS, with a flow of 1000 mL/min monitored by a Type πMFC Digital Mass Flow Controller (Model PFC-50, MKS Instruments). A high voltage AC power supply (Trek PM04015) biased the inner electrode during experiments at 12 kV (peak to peak) and 1000 Hz, while the outer electrode remained grounded. Between the power supply

and the tungsten filament, there is a 1 MΩ resistor used as a current limiter. A low temperature plasma (dielectric barrier discharge) is generated inside the tube, producing hydroxyl radicals in the gas flow. Compared to the tropospheric OH radical concentration that was measured to be 1-3 × 10^6 molecules cm^{-3},[29] the DBDS can generate ~1×10^9 molecules cm^{-3} OH radicals based on the time required to oxidize a monolayer of surfactant with an average of one oxygen per surfactant molecule. This significantly accelerates the oxidation process compared to ambient conditions.

2. Results and discussion

3.1. Oxidation product analysis by mass spectrometry

Figure 1 presents the mass spectra of the OH oxidation products of OA at the air-water interface. The time periods each droplet was exposed to OH radicals are 0 s, 15 s, 30 s and 60 s. The deprotonated OA monomer and dimer are observed at *m/z* 281 and *m/z* 563, respectively. As oxidation proceeds, the intensity of the dimer relative to the monomer increases in the FIDI mass spectra. This may indicate increased attraction of the oxygenated monomers resulting in an increase in the in the amount of dimer that is eventually detected during the sampling process, which is analogous to the process of ion formation in electrospray ionization. In Figure 1, the peaks appearing over time at *m/z* values above the monomer and the dimer are the oxidation products. Each group of peaks represents products adding one, two or more oxygen atoms to the parent anions. The postulated structures and mechanisms of formation of the major oxygenated products are discussed below. By increasing the oxidation time, the relative intensity of the products increases relative to the remaining unreacted precursors. At lower mass range, starting from *m/z* 171 and beyond, products attributed to C=C double bond cleavage processes can be observed. However, their intensities are very low (less than 5% of all the products and reactants

after 60 s oxidation), which is very different from the OA ozonolysis reactions, where the C=C double bond cleavage products dominate.[13] There is no evidence observed for either radical or nitrogen containing products in the spectra.

Based on the analysis of the peaks in Figure 1, the average number of oxygen atoms per molecule as a function of time is shown in Figure 2. The amount of oxygen incorporation increases linearly with time, resulting in an average of one oxygen atom per oleic acid at 20 sec. Assuming an accommodation coefficient in the range 0.3 – 0.5 the observed rate of oxidation is consistent with a gas phase concentration of OH radicals around 10^9 cm^{-3}, three orders of magnitude above ambient values. The linear behavior suggests Langmuir-Hinshelwood kinetics[30] where OH accommodated at the surface eventually reacts to yield oxidized products. If accommodated OH desorbed back to the gas phase, or if OH reacted directly on contact with the surfactant layer (Eley-Rideal kinetics), it would be expected that the data in Figure 2 would exhibit an upward curvature, resulting from the introduction of weaker, more reactive C-H bonds in the exposed molecules as oxidation proceeds.

Figure 3 demonstrates the occurrence of exchange between the oxidized species at the interface and the unreacted subsurface excess oleic acid in the solution. After being oxidized for 30 s, the FIDI-MS spectrum of oxidized OA is sampled following a 90 s time delay (lower spectrum in Figure 3). Compared to sampling with no delay (upper spectrum in Figure 3), this results in a significant decrease in oxidized OA yields, which indicates diffusion of the now more hydrophilic oxidized species into solution in exchange for unoxidized excess subsurface oleic acid. The diffusion likely occurs at different rates for different oxidized products, making it problematic to extract rate data for individual steps in the competing and sequential oxidation processes. This is likely responsible for making it seem that many of the product peaks all

appear at once rather than exhibiting the expected increase in abundance of the more highly oxidized products over time. In earlier FIDI studies of the oxidation of lipid mixtures by ozone it was observed that eventually the products from oxidized unsaturated lipids were dissolved back into solution, leaving a surface layer dominated by unreactive saturated lipids.[26] Ozone reacts only with sites of unsaturation in lipids.

Expanded views of the mass spectra showing the major oxidation products of OA are presented in Figure 4. Both the products and their distributions are reproducible from day to day experiments. For the OA monomer, the major product is adding one oxygen atom, 16 Da more than the parent anion, and there is also a smaller adding 14 Da peak. The most abundant products adding two, three and four oxygen atoms are in turn 16, 14, and 16 Da heavier. For the dimer of the oxidized monomers, four major adding 16 Da peaks show up before the adding 14 peak, a result of dimer formation of the doubly oxidized monomer. Since gas phase reaction rate constants of OH oxidation of alkenes are usually one or two orders of magnitude higher than that of OH oxidation of alkanes,[11, 31-33] we assume that not until all of the C=C double bonds of OA are "consumed" by the OH radicals can the saturated carbon atoms play a major role in the reactions. We conclude that the first two adding 16 Da peaks (*m/z* 297 and 313) in the monomer are due to the reactions of the double bond, while the latter adding 14 Da (*m/z* 327) and adding 16 Da (*m/z* 343) peaks are from the oxidation of the saturated carbon atoms. Some of the minor products indicated by less intense peaks such as *m/z* 295 and *m/z* 311 are likely due to the oxidation of saturated alkyl groups (*vide infra*).

Figure 5 presents an expanded view of the low abundance C-C bond cleavage products of OH oxidation of OA after 15 and 60 s. This series begins from *m/z* 171, and continues with combinations of adding 14 and 16 Da. Note that the intensities of these bond cleavage products

are much lower than other products discussed above (Figures 1 and 4) where no bond cleavage occurs; they amount to approximately 4% of the total product yield. The major *m/z* 171 peak is a result of the C=C bond cleaved into an aldehyde group, and the peaks at higher *m/z* can be accounted for as oxidation products of the nascent aldehyde product.

Figure 6 presents an expanded view of the OH oxidation products of the stearic acid molecule, which is identical to oleic acid absent the double bond. In contrast to oleic acid, the first major product is adding 14 Da to the stearic acid molecule, and the second product is further adding 16 Da. Products at higher m/z are combinations of adding 14 Da and 16 Da.

3.2. Proposed Reaction Mechanisms

We next discuss the possible reaction mechanisms for generating the observed oxidation products. In Scheme 1 and 2, all of the species marked by red boxes are those observed in the mass spectra and the reaction steps are marked by (1), (2) etc.

3.2.1 OH oxidation of the C=C double bond

Scheme 1 illustrates the proposed oxidation mechanism of the double bond. Step (1) is the uptake of one OH radical from the gas phase by the double bond, forming a β-hydroxyalkyl radical. This OH addition is a well-accepted reaction of OH and alkenes.[11,18] In the current study, we assume that the OH prefers to attach to the ω−10 carbon because it is closer to the gas phase than the ω−9 carbon is. Afterwards, the hydroxyalkyl radical generated in step (1) could uptake an O_2 molecule to form a hydroxyperoxy radical in step (2) since the concentration of ambient O_2 is many orders of magnitude higher than OH. The peroxy moiety could abstract an H atom on the ω−10 carbon, resulting in an HO_2 leaving group and an enol product (step (3)). This HO_2 forming step was also observed in the reaction between OH and benzene in the presence of O_2.[34]

The enol product can undergo step (4), the enol-keto tautomerization, to form a more stable carbonyl group on the ω−10 carbon, this being the *m/z* 297 product. Our result is different from the OH oxidation of unsaturated fatty acid solid particles where reactions between two adjacent molecules were observed,[18,19] this might be because the OA molecules are more densely packed in a particle than at the air-water interface. An alternative to the process proposed for formation of the m/z 297 product would be the direct abstraction of the alpha hydrogen by O_2 to yield the enol product.

As demonstrated by previous condensed phase studies,[35-37] the hydroxyperoxy radical formed in step (2) could react with another hydroxyperoxy radical to form a tetroxide intermediate, which will further rapidly decay into two hydroxylalkoxy radicals and one O_2 molecule. However, this intermediate is very unstable if formed at all. Therefore, we adopt another well-known mechanistic step that involves NO.[38,39] The NO concentration in Los Angeles area is typically ~1×10^{11} molecules cm^{-3},[40] significantly higher than the OH concentration in the current study, so it is reasonable to include NO in the mechanistic step (5). NO will abstract an oxygen atom from the peroxy group to yield a hydroxylalkoxy radical and NO_2. From this hydroxyalkoxy radical, two different reactions could occur: it could either react with an O_2 molecule to form a hydroxyketone (step (6), *m/z* 313) and an HO_2 leaving group, or undergo a unimolecular dissociation to form an aldehyde (step (7), *m/z* 171) and an hydroxyalkyl. Both step (6) and step (7) are very well documented reaction pathways in the reactions of OH and hydrocarbons.[39,41,42] The aldehyde resulting from step (7) can further be oxidized into a carboxylic acid as shown in step (8), which is accountable for the *m/z* 187 product (Figure 5). In Figure 5, the less intense peaks beyond *m/z* 171 and *m/z* 187 involve further oxidation of the remaining saturated alkyl groups in the molecule.

3.2.2 OH oxidation of the saturated alkyl groups

After the more reactive C=C double bonds are "consumed" by the OH radicals, the remaining saturated alkyl groups in OA are ready to be oxidized. In Scheme 2, we start from the *m/z* 313 reactant, the product from the OH oxidation of the C=C double bond. The reaction starts with an H atom abstraction by an OH radical, resulting in an alkyl radical. Then it follows step (2) to step (4) to form a carbonyl group, which are very similar to steps (5) and (6) in Scheme 1. This carbonyl group containing product is 14 Da more than the reactant, and can account for the *m/z* 327 product. The alkoxy radical could also undergo an isomerization (hydrogen atom transfer) through a six-member ring, ending up as a γ-hydroxyalkyl radical. This radical can repeat step (2) to step (4) to form another carbonyl group, this being accountable for the *m/z* 343 product, 16 Da more than the *m/z* 327 product. Therefore, OH oxidation of saturated alkyl groups prefers to follow this adding 14 Da and then adding 16 Da pattern. With this knowledge, we look back on the smaller *m/z* 295 and *m/z* 311 peaks in Figure 4, they follow this +14 and +16 oxidation pattern. They are actually the oxidation products of the saturated alkyl groups of OA.

The mechanism of OH oxidation of saturated alkyl groups can be further testified by the oxidation of stearic acid, which follows the adding 14 and then adding 16 Da pattern (Figure 6).

The initial introduction of hydroxyl and carbonyl groups into saturated and unsaturated hydrocarbons creates sites where weakened C-H bonds are more likely to react further with OH by hydrogen abstraction and subsequently with O_2 and NO in accordance with Scheme 2. This ultimately leads to highly oxidized products, such as observed in Figure 4 and Figure 6.

3. Conclusion

We have presented the OH oxidation reactions of OA at the air-water interface using FIDI-MS, a technique that is interface-sensitive and capable of online sampling of the reaction products. Unlike previously reported data on the oxidation of solid particles of unsaturated fatty acids,[18] our results show that the OH oxidation of the C=C double bond results in bond cleavage products (minor), and major products adding 16 Da, representing a carbonyl group, and adding 32 Da, representing a combination of a carbonyl group and a hydroxyl group. Following the reactions involving the double bond, OA can further be oxidized on the saturated carbon atoms, which follows a pattern involving addition of 14 Da (carbonyl) and then 16 Da (hydroxyl). This same pattern is observed in the oxidation of stearic acid, for which the double bond is absent. In the proposed mechanisms, OH is the reaction initiator, but ambient O_2 and NO play important roles in generating the final observed products. Even though the oxidation mechanisms are different for the unsaturated and saturated hydrocarbons, the oxidation products are similar in both cases, representing combinations of carbonyl groups and hydroxyl groups added to the hydrocarbon chain. As oxidation proceeds the increasingly hydrophilic products are observed to exchange with unreacted subsurface molecules on a one minute time scale.

Acknowledgement

This work was supported by the Beckman Institute at Caltech and by the NSF grants CHE-1508825.

References

[1] M. Grossi, G.D. Lecce, T.G. Toschi, B. Riccò, *IEEE Sens. J.* **14** (2014) 2947–2954.

[2] J.E. Villarreal-Lozoya, L. Lombardini, L. Cisneros-Zevallos, *Food Chem.* **102** (2007) 1241–1249.

[3] M.K. Nutter, E.E. Lockhart, R.S. Harris, *Oil & Soap* **20** (1943) 231–234.

[4] M.G. Kokatnur, M.C. Oalmann, W.D. Johnson, G.T. Malcom, J.P. Strong, *Am. J. Clin. Nutr.* **32** (1979) 2198–2205.

[5] R.E. Peterson, B.J. Tyler, *Appl. Surf. Sci.* **203** (2003) 751.

[6] J.C. Marty, P. Saliot, P. Buat-Ménard, R. Chesselet, K.A. *J. Geophys. Res.* **84** (1979) 5707–5716.

[7] H. Tervahattu, K. Hartonen, V.-M. Kerminen, K. Kupiainen, P. Aarnio, K. Koskemtalo, A.F. Tuck, V. Vaida, *J. Geophys. Res.* 107 (2002) 4053.

[8] H. Tervahattu, J. Juhanoja, K. Kupiainen, *J. Geophys. Res.* **107** (2002) 4319.

[9] W.F. Rogge, L.M. Hildemann, M.A. Mazurek, G.R. Cass, B.R.T. Simoneit, *Environ. Sci. Technol.* **25** (1991) 1112–1125.

[10] K. Siegmann, K. Sattler, *J. Aerosol Sci.* **27** (1996) S493-S494.

[11] R. Atkinson, J. Arey, *Chem. Rev.* 103 (2003) 4605-4638.

[12] I.S.A. Isaksen, S.B. Dalsøren. *Science* **331** (2011) 38–39.

[13] R.L. Grimm, R. Hodyss, J.L. Beauchamp, *Anal. Chem.* **78** (2006) 3800-3806.

[14] L.F. Voss, M.F. Bazerbashi, C.P. Beekman, C.M. Hadad and H.C. Allen, *J. Geophys. Res.* **112** (2007) D06209/1-D06209/9.

[15] E. González-Labrada, R. Schmidt, C.E. DeWolf, *Phys. Chem. Chem. Phys.* **9** (2007) 5814-5821.

[16] M.D. King, A.R. Rennie, K.C. Thompson, F.N. Fisher, C.C. Dong, R.K. Thomas, C. Pfrang, A.V. Hughes, *Phys. Chem. Chem. Phys.* **11** (2009) 7699-7707.

[17] Z. Zhao, S. Husainy, C.T. Stoudemayer, G.D. Smith, *Phys. Chem. Chem. Phys.* **13** (2011) 17809-17817.

[18] T. Nah, S.H. Kessler, K.E. Daumit, J.H. Kroll, S.R. Leone, K.R. Wilson, *Phys. Chem. Chem. Phys.* **15** (2013) 18649-18663.

[19] T. Nah, S.H. Kessler, K.E. Daumit, J.H. Kroll, S.R. Leone, K.R. Wilson, *J. Phys. Chem. A* **118** (2014) 4106−4119.

[20] G.D. Smith, E. Woods, III, C.L. DeForest, T. Baer, R.E. Miller, *J. Phys. Chem. A* **106** (2002) 8085-8095.

[21] K.S. Docherty, P.J. Ziemann, *J. Phys. Chem. A* **110** (2006) 3567-3577.

[22] H.-M. Hung, Y. Katrib, S.T. Martin, *J. Phys. Chem. A* **109** (2005) 4517-4530.

[23] Y. Katrib, S.T. Martin, H.-M. Hung, Y. Rudich, H. Zhang, J.G. Slowik, P. Davidovits, J.T. Jayne, D.R. Worsnop, *J. Phys. Chem. A* **108** (2004) 6686–6695.

[24] R.L. Grimm, J.L. Beauchamp, *J. Phys. Chem. B* **107** (2003) 14161-14163.

[25] H.I. Kim, H.J. Kim, Y.S. Shin, L.W. Beegle, S.S. Jang, E.E. Neidholdt, W.A. Goddard, J.R. Heath, I. Kanik, J.L. Beauchamp, *J. Am. Chem. Soc.* **132** (2010) 2254-2263.

[26] H.I. Kim, H.J. Kim, Y.S. Shin, L.W. Beegle, W.A. Goddard, J.R. Heath, I. Kanik, J.L. Beauchamp, *J. Phys. Chem. B* **114** (2010) 9496-9503.

[27] J.Y. Ko, S.M. Choi, Y.M. Rhee, J.L. Beauchamp, H.I. Kim, *J. Am. Soc. Mass Spectrom.* **23** (2012) 141-152.

[28] R.L. Grimm, J.L. Beauchamp, *J. Phys. Chem. B* **109**, (2005), 8244-8250.

[29] G. Hübler, D. Perner, U. Platt, A. Tönnissen, D. H. Ehhalt, *J. Geophys. Res.* **89** (1984) 1309-1319.

[30] M. Ammann, U. Pöschl and Y. Rudich, *Phys. Chem. Chem. Phys.* **5** (2003) 351-356.

[31] R. Atkinson, *Atmos. Chem. Phys. Discuss.* **3** (2003) 4183.

[32] R. Atkinson, *J. Phys. Chem. Ref. Data* **26** (1997) 215.

[33] J.G. Calvert, R. Atkinson, J.A. Kerr, S. Madronich, G.K. Moortgat, T.J. Wallington, G. Yarwood, *The Mechanisms of Atmospheric Oxidation of the Alkenes*. Oxford University Press, New York, 2000.

[34] S. Nehr, B. Bohn, H. Fuchs, A. Hofzumahaus, A. Wahner, *Phys. Chem. Chem. Phys.* **13** (2011) 10699-10708.

[35] K.U. Ingold, *Acc. Chem. Res.* **2** (1969) 1–2.

[36] C. von Sonntag, H.P. Schuchmann, *Angew. Chem., Int. Ed. Engl.* **30** (1991) 1229–1253.

[37] C. von Sonntag, P. Dowideit, X.W. Fang, R. Mertens, X.M. Pan, M.N. Schuchmann and H.P. Schuchmann, *Water Sci. Technol.* **35** (1997) 9–15.

[38] M.D. King, K.C. Thompson, *Atmos. Environ.* **37** (2003) 4517-4527.

[39] J. Calvert, R.G. Derwent, J.J. Orlando, G.S. Tyndall, T.J. Wallington. *Mechanisms of atmospheric oxidation of the alkanes.* OUP, USA, 2008.

[40] D. Westerdahl, S. Fruin, T. Sax, P.M. Fine, C. Sioutas, *Atmos. Environ.* **39** (2005) 3597-3610.

[41] B.J. Finlayson-Pitts, J.N. Pitts, Jr. *Chemistry of the Upper and Lower Atmosphere*. Academic press, USA, 1999.

[42] J.G. Calvert, R. Atkinson, J.A. Kerr, S. Madronich, G.K. Moortgat, T.J. Wallington, G. Yarwood, *The mechanism of atmospheric oxidation of the alkenes.* Oxford University Press, UK, 2000.

Figure Captions.

Figure 1. Time-resolved FIDI-MS spectra including the reactant and products of the reaction between OA and OH radicals. The monomer and proton bound dimer of deprotonated OA appear at *m/z* 281 and 563. Low abundance bond cleavage products are observed starting at *m/z* 171.

Figure 2. The average number of incorporated oxygen atoms per OA molecule as a function of time. A linear increase is noted, suggestive of Langmuir-Hinshelwood kinetics.

Figure 3. The 0 s and 90 s time delays prior to FIDI-MS sampling illustrates the effect of diffusion on the relative abundance of oxidation products observed at the air-water interface. After 30 s of OH oxidation, the decrease in oxidized OA intensity following a 90 s delay before sampling is indicative of the diffusion of the more hydrophilic oxidized species into solution, in exchange for unreacted subsurface excess oleic acid.

Figure 4. Expanded view of the OH oxidation products after 60 s, corresponding to the monomer (upper spectrum) and dimer (lower spectrum) of oxidized OA.

Figure 5. Expanded view of the low mass OH oxidation bond cleavage products of OA after oxidation of 15 s and 60 s.

Figure 6. FIDI-MS spectrum showing OH oxidation products of deprotonated stearic acid monomer after oxidation for 15 s.

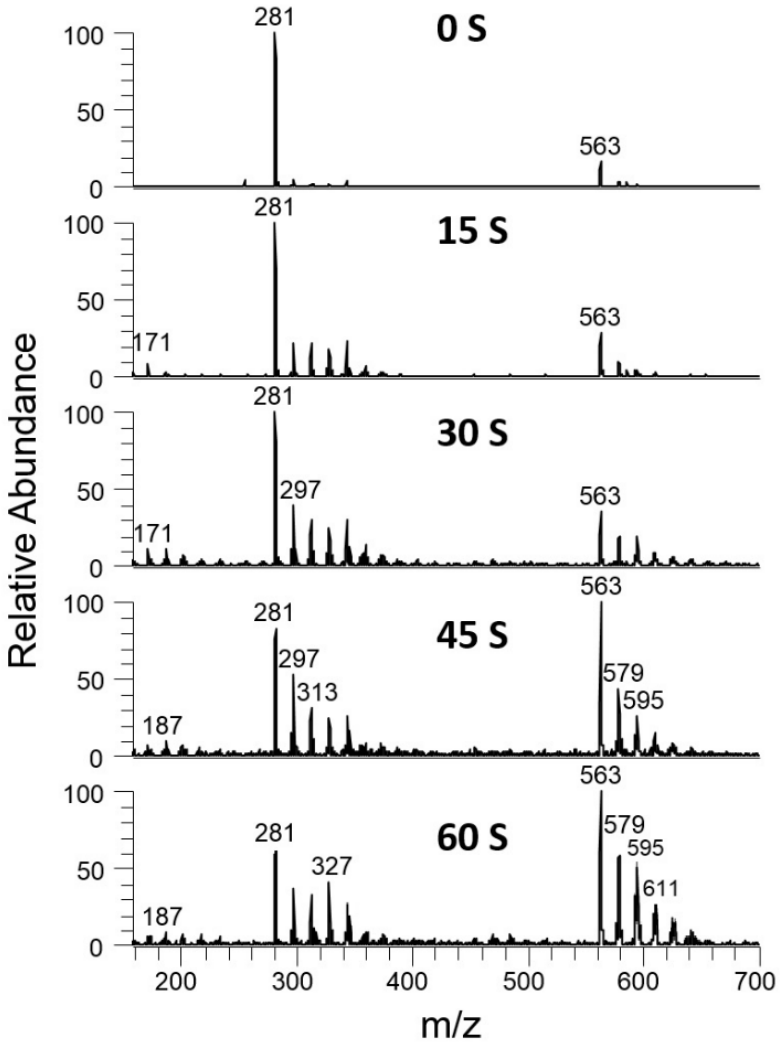

Figure 1

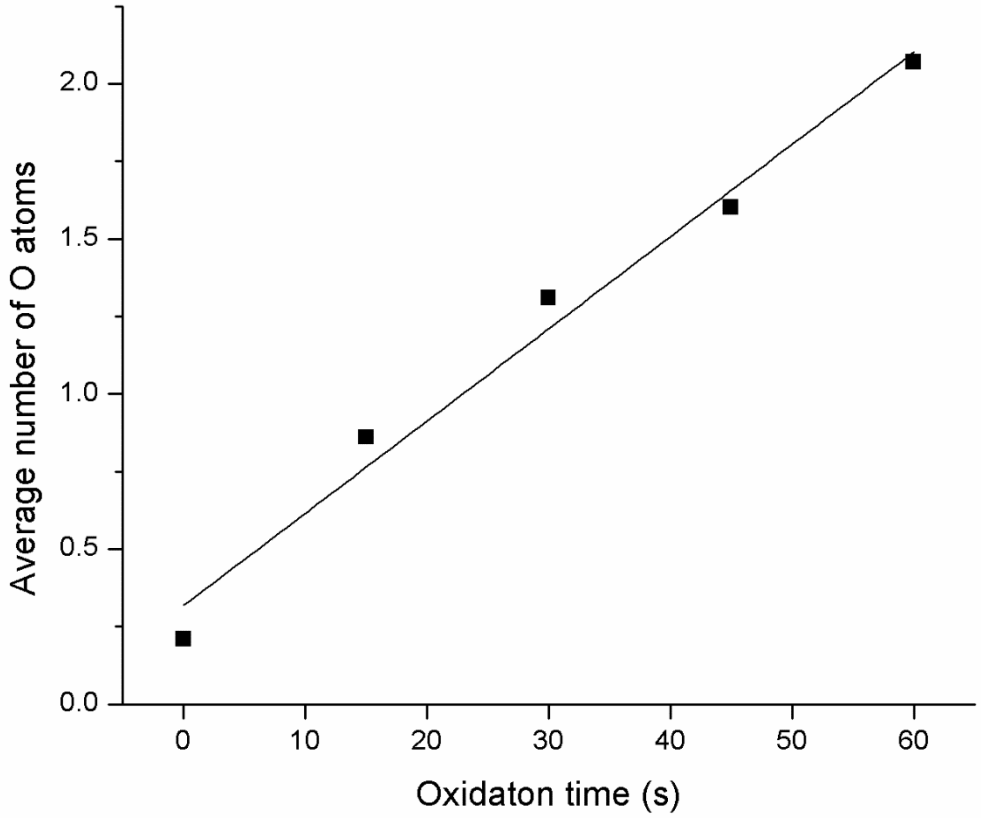

Figure 2

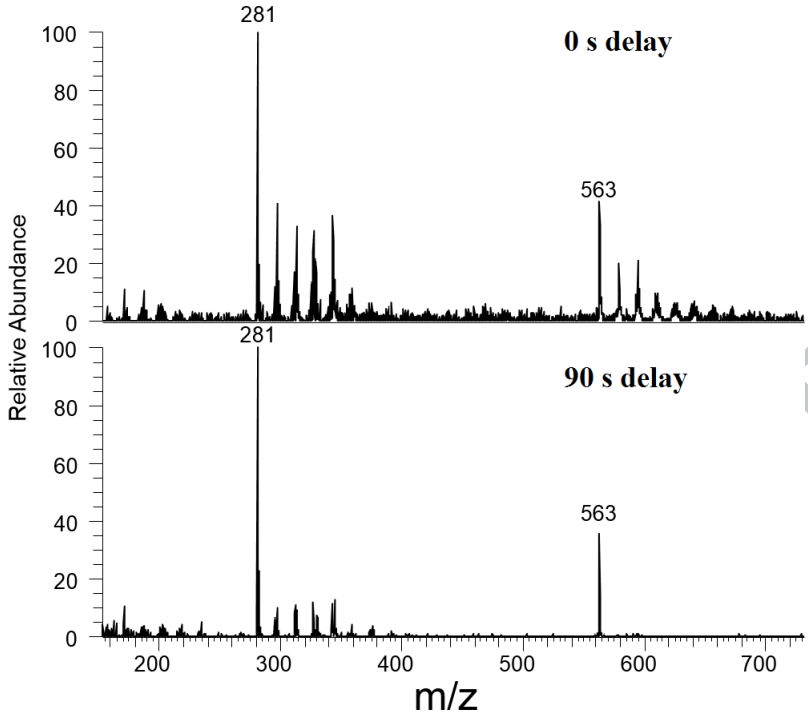

Figure 3

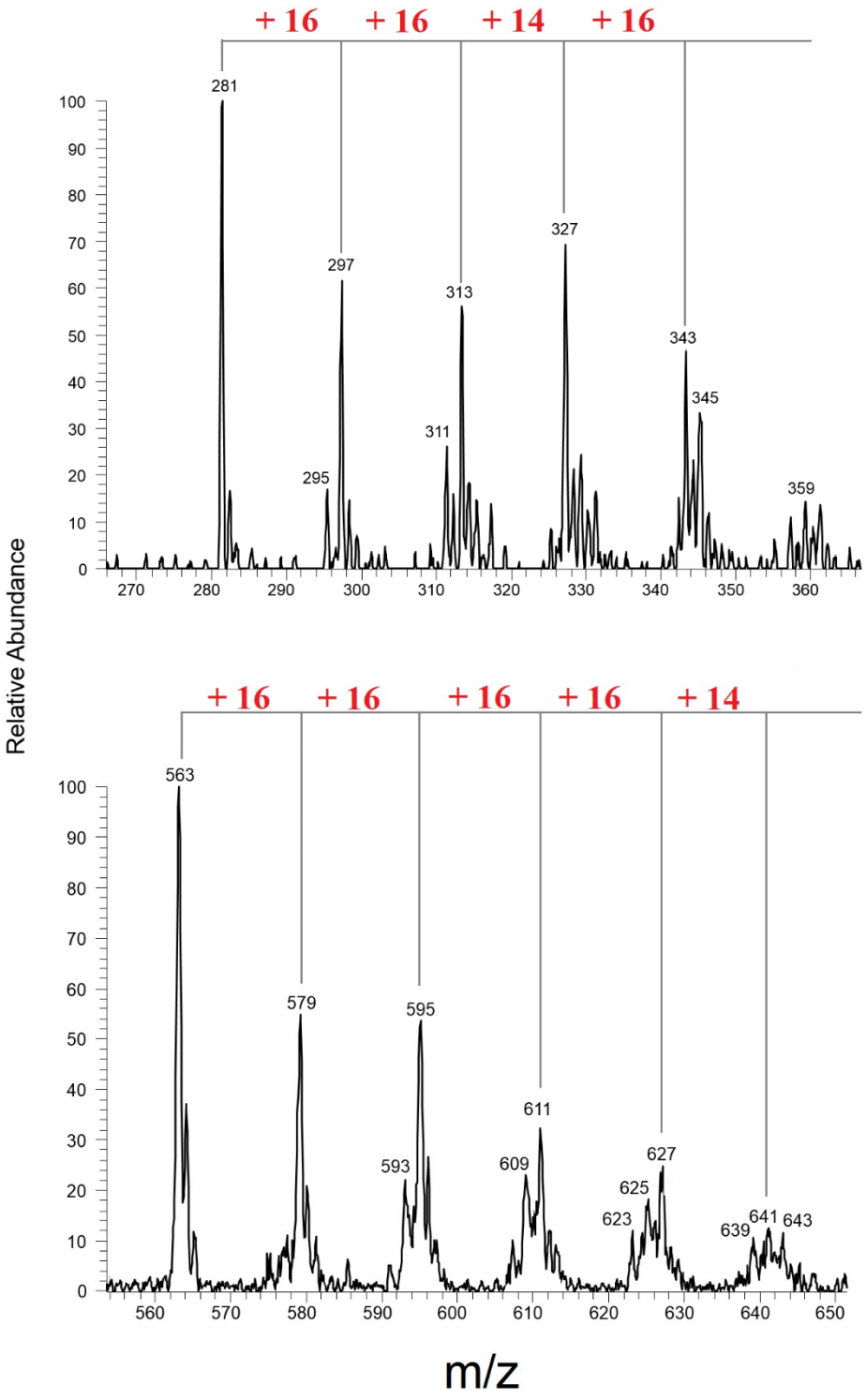

Figure 4

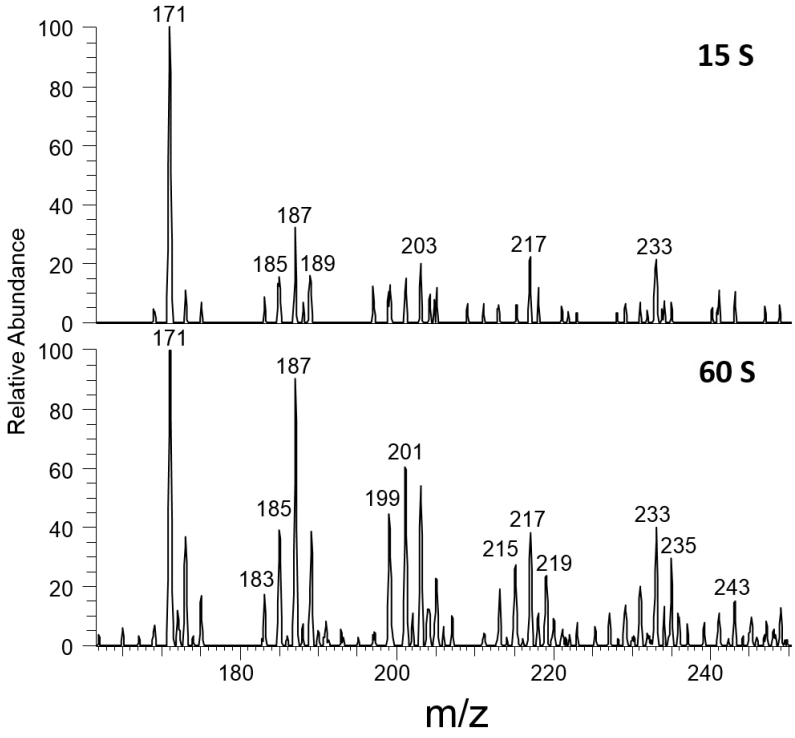

Figure 5

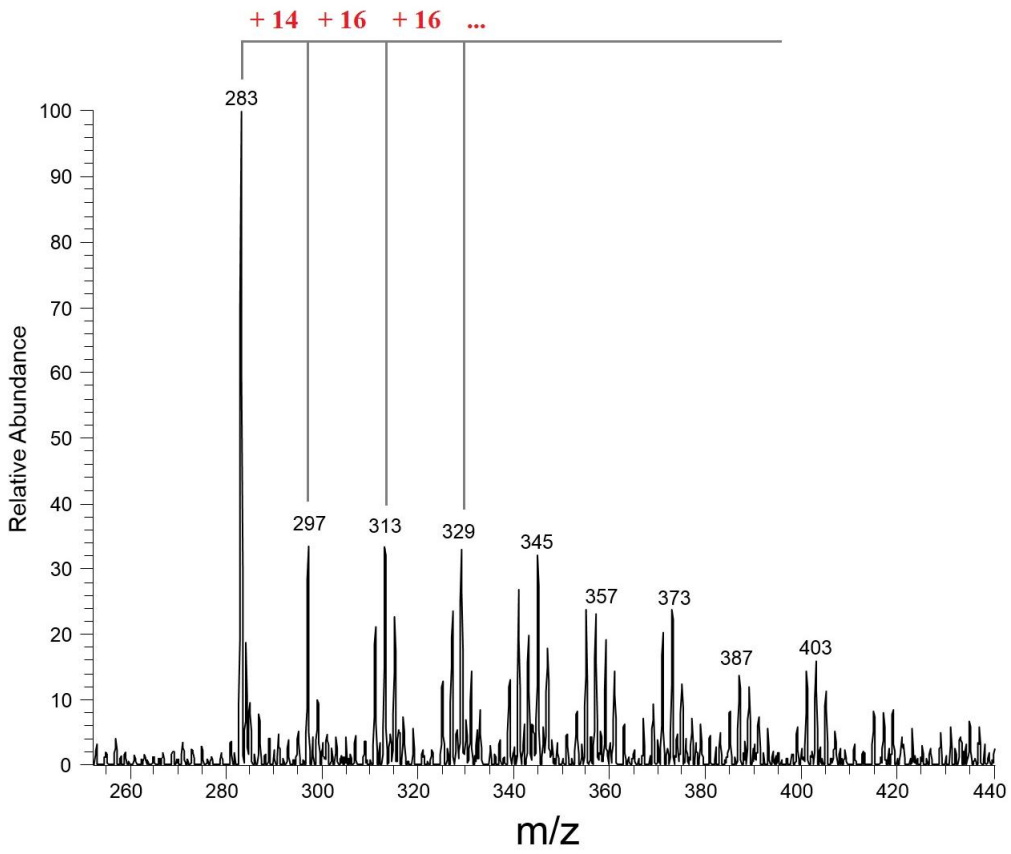

Figure 6

Scheme Captions.

Scheme 1. Proposed mechanism of the OH oxidation of the unsaturated C=C bond of oleic acid.

Scheme 2. Proposed mechanism of the OH oxidation of the saturated alkyl groups of oleic acid.

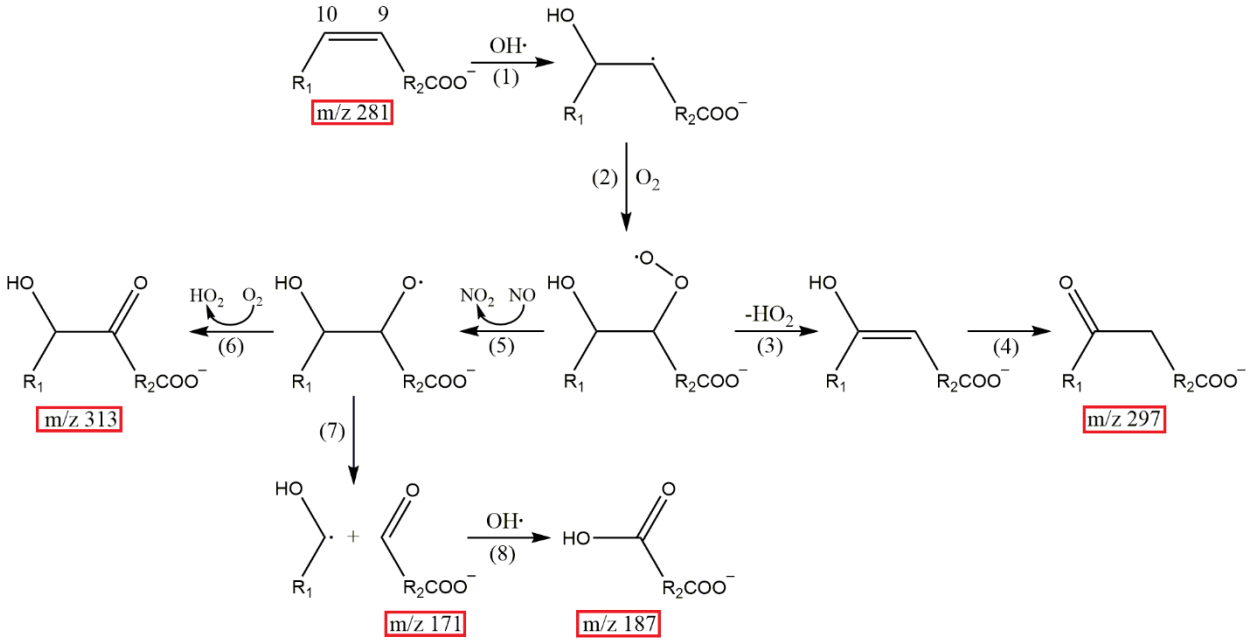

Scheme 1

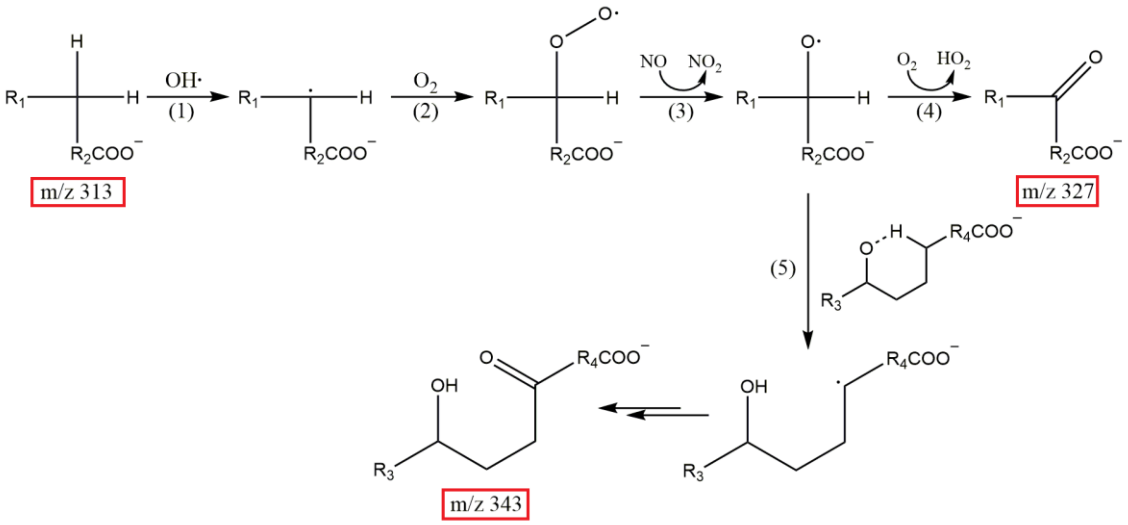

Scheme 2

Graphical abstract

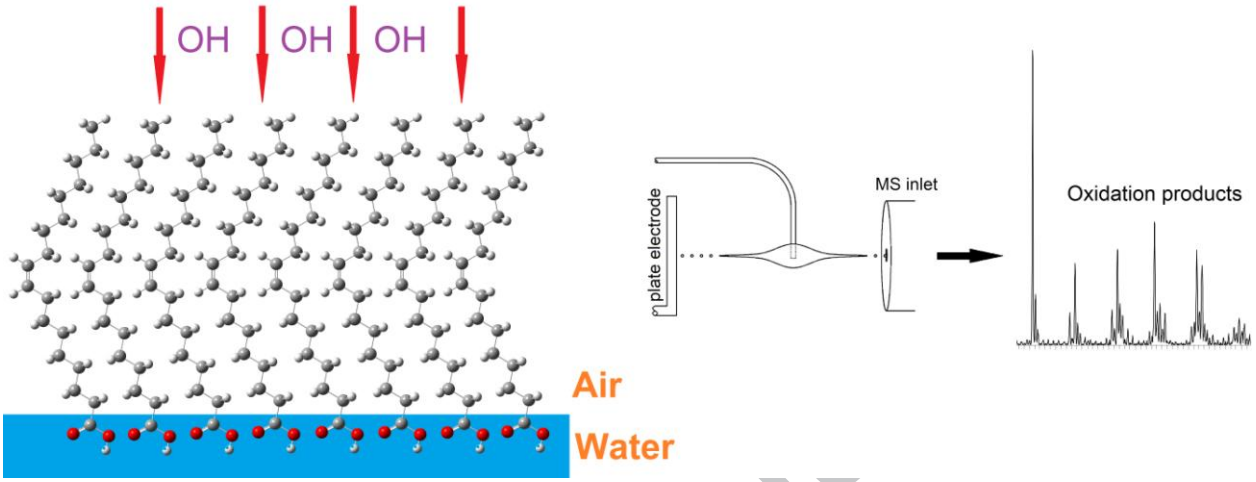

Highlights

- OH oxidation of oleic acid is studied at the air-water interface.
- OH oxidation of stearic acid is studied at the air-water interface.
- OH oxidation mechanisms are proposed for both cases.